Supplementary Information

Complex Coordination of Multi-Scale Cellular Responses to Environmental Stress

Luís L. Fonseca, Claudia Sánchez, Helena Santos and Eberhard O. Voit

---

Contents

Glucose uptake dynamics

Our *in vivo* experiments suggest that the glucose consumption kinetics by yeast cells depends on the surrounding temperature. In order to explore these differences quantitatively, we developed a model that addresses different transport characteristics for α- and β-glucose anomers as well as the process of anomerization. The consumption of each anomer was individually represented as Michaelis-Menten kinetics, with the result

$$\frac{d}{dt}\begin{bmatrix}\alpha Glc\\ \beta Glc\end{bmatrix}=\begin{bmatrix}-A\cdot\dfrac{V_{\max}^{\alpha Glc}\cdot\alpha Glc}{K_m^{\alpha Glc}+\alpha Glc}-k_{\alpha\beta}\cdot\alpha Glc+k_{\beta\alpha}\cdot\beta Glc\\ -A\cdot\dfrac{V_{\max}^{\beta Glc}\cdot\beta Glc}{K_m^{\beta Glc}+\beta Glc}+k_{\alpha\beta}\cdot\alpha Glc-k_{\beta\alpha}\cdot\beta Glc\end{bmatrix}$$

[1]. Here, V_{max} and K_m are the maximal velocity and the Michaelis constant for the transport of each anomer, while $k_{\alpha\beta}$ and $k_{\beta\alpha}$ are the first-order rates of anomerization of α- into β- and of β- into α-anomers, respectively. Since the first-order rates are temperature dependent, they were determined for both temperatures as $k_{\alpha\beta}(30)$ = 0.1077 min^{-1}, $k_{\alpha\beta}(39)$=0.3051 min^{-1}, $k_{\beta\alpha}(30)$= 0.06267 min^{-1}, and $k_{\beta\alpha}(39)$=0.1906 min^{-1}. The first-order rate constants of glucose anomerization were determined by monitoring the anomerization of a 20 mM solution of α-[1-^{13}C]-glucose dissolved in the same buffer that was used for the *in vivo* NMR experiments (50 mM KPi, pH 6.5), at 30°C and at 39°C by ^{13}C-NMR. The data were then used to fit a model similar to the one above, but without glucose consumption. The V_{max} for glucose consumption was calculated as the sum of the V_{max} values for the two anomers. We are currently developing statistical methods for quantifying generically whether differences between two uptake curves are significant.

Immediately after adding the glucose pulse, glucose consumption does not proceed at its maximum rate as expected for a Michaelis-Menten process. This deviation can have a biological origin. For instance, de-energized cells that are not able to transport the substrate at maximal capacity, could require a short period of time to become fully energized and achieve maximum substrate consumption. The deviation from a Michaelis-Menten rate-law could also stem from the experimental system set-up: the cell suspension is pumped through the NMR apparatus with 2-meter long thin tubes. As a consequence, non-zero mixing times are likely to occur, with special relevance during the first one or two minutes of glucose consumption. This effect can be modeled by incorporating into the Michaelis-Menten process a time dependent factor A, which increases linearly for two minutes as $A = a \cdot t + b$ (a>0 and 0<b<1)

until saturation at A=1. While we did not use this module for our analysis directly, we used it to calculate the maximum capacity of glucose consumption at the two temperatures examined (30 °C and 39 °C).

Glucose 6-phosphate pool

Given the strong increase in the pool of trehalose in response to heat stress, we deemed it important to determine whether this result was associated with a putative increase in the size of the glucose 6-phosphate (G6P) pool. Therefore, we set out to measure the dynamics of this metabolite *in vivo*. Unfortunately, the nuclear magnetic resonances due to [1-^{13}C]glucose and [1-^{13}C]G6P overlap significantly, and the small G6P signal is obscured by the much larger [1-^{13}C]glucose signal. This issue can be overcome by utilizing glucose labeled on a carbon atom other than C1, such as [6-^{13}C]glucose. Indeed the results from a [6-^{13}C]glucose experiment show that G6P accumulation is similar to that of FBP, both in magnitude and duration, and that it is unaffected by an increase in temperature from 30ºC to 39ºC (Figure S1). Thus, a larger G6P pool is not the source of the increase in trehalose under heat conditions.

Trehalose degradation

The degradation patterns of different pulses of trehalose, best seen in Figure 2 but also in Figure 1 of the Text, are intriguing. It seems as if the two boluses are degraded independently of each other. No definite explanation can be given at present, but a brief model analysis shows that the observations are consistent with the following hypothesis.

Suppose the generated trehalose can be free (TF) or bound (TB) to intracellular structures, such as membranes, and that the enzyme trehalase (E) can only degrade TF. Suppose further that the association (binding) constant k_a is normally much smaller than the dissociation constant k_d, which itself has a low value. If so, most trehalose will be free under optimal

temperature, and the degradation of trehalose follows a Michaelis-Menten-like process. Now suppose that k_a is strongly increased under heat conditions, such that it becomes much larger than k_d. As a consequence, most trehalose will become bound and only slowly turn into the free form, due to the slow dissociation with an unchanged, small constant k_d. Because of the small concentration of TF, the degradation process is substrate limited and essentially independent of E. Indeed, the free substrate concentration is governed by the small k_d and is more or less constant, as there is a lot of TB. A second trehalose pulse under heat stress leads to twice as much TB and therefore to roughly a doubled amount of $k_d \times$TB that becomes free trehalose and can be degraded. As a result, it appears that both trehalose pulses are degraded independently (see Figure 2). By contrast, if the second trehalose pulse is given under cold conditions, it is immediately degraded according to a Michaelis-Menten-like process, while the "old" trehalose is still mostly bound (see Figure 1).

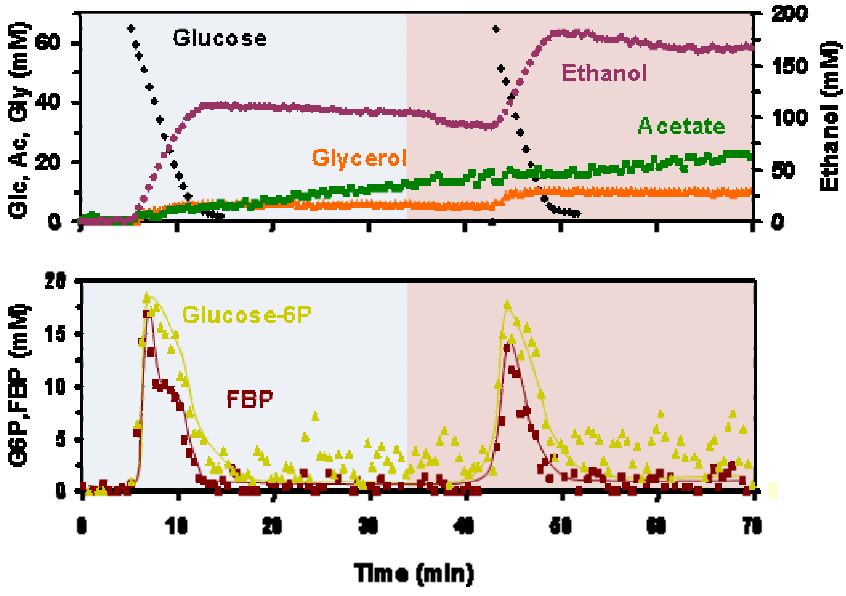

Figure S1 Metabolite time courses of glucose metabolism determined by *in vivo* ^{13}C-NMR in *Saccharomyces cerevisiae* grown under optimal temperature. Two consecutive pulses of [6-^{13}C]glucose were supplied under different temperatures: 30ºC ( ); 39ºC ( ). Experimental data are shown for glucose (◆) ethanol (●), glycerol (▲), acetate (■), FBP (■) and glucose 6-phosphate (▲). Lines visualize the trends in FBP and glucose 6-phosphate.

Because intuition is easily prone to failure, we formulated this hypothesis as a small model with arbitrary units (Box S1), which can be directly copied and pasted into in PLAS [2]. Model simulations of the different scenarios reflect the observations quite well. Figure S2A corresponds to Figure 2 in that the second bolus is given under heat stress, while Figure S2B corresponds to Figure 1, where the second bolus is given under cold conditions.

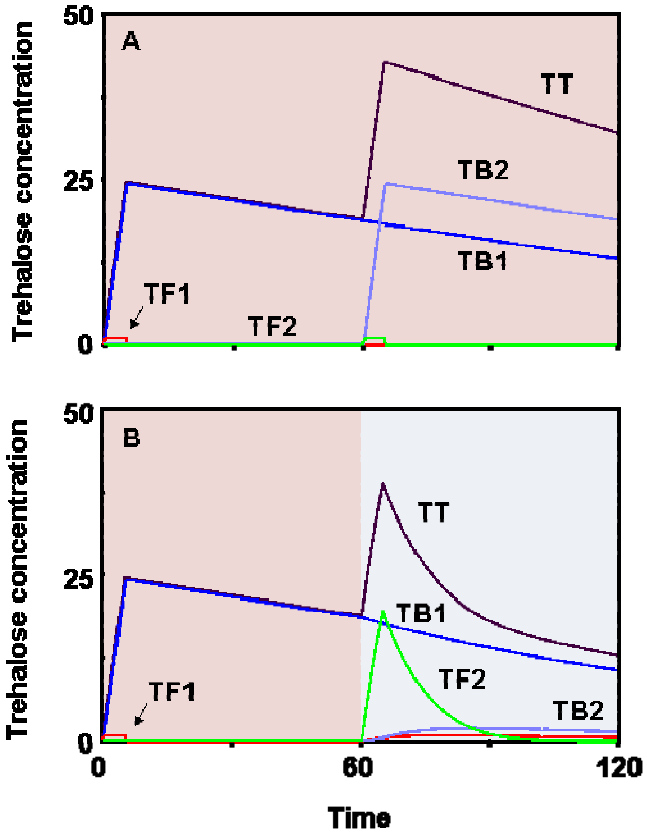

Figure S2 Model simulation of trehalose degradation under the hypothesis of free (TF) and bound (TB) trehalose. Two boluses were administered (indicated by 1 and 2) and TF, TB, and total trehalose (TT) were plotted. Panel A corresponds to Figure 2 and represents the situation where both boluses are given under heat stress, while panel B corresponds to Figure 1, where the second bolus is given under cold conditions.

Box S1: PLAS file for testing the hypothesis of free and bound trehalose

```
TB1' = ka TF1 - kd TB1 + BolusB1
TF1' = kd TB1 - ka TF1 + BolusF1 – 0.15 E TF1^h11
TB1 = 0.1
TF1 = 0.1

TB2' = ON (ka TF2 - kd TB2 + BolusB2)
TF2' = ON (kd TB2 - ka TF2 + BolusF2 - 0.15 E TF2^h11)
TB2 = 0.1
TF2 = 0.1
TT = TF1 + TB1 + TF2 + TB2

ka = 5
kd = 0.01
E = 1
h11 = 0.1

ON = 0
BolusB1 = 0
BolusF1 = 5
BolusB2 = 0
BolusF2 = 0
t0 = 0
tf = 120
hr = .1

@ 5 BolusF1 = 0
@ 60 ON = 1
@ 60 BolusF2 = 5
@ 65 BolusF2 = 0
..@ 60 ka = 0.01        // for cold conditions
..@ 60 h11 = 0.8        // these two statements have to be activated
```

Comments:

1. TB = bound Trehalose; TF = free Trehalose; TT = total Trehalose
2. For cold conditions: ka = 0.01; kinetic order of trehalose degradation h11= 0.1
3. For heat stress: ka = 5; kinetic order of trehalose degradation h11= 0.8
4. The system starts under heat stress
5. At t=60, the temperature switches from hot to cold
6. The two periods in the last two statements must be removed for a second bolus under heat stress

Temperature profiles of enzyme activities

Neves and François [3] reported that the three enzymes directly associated with the trehalose cycle are dependent on temperature (Figure S3). We set out to answer the question of whether the heat response could be due exclusively to changes in these three enzymes. Our dynamic model results showed that the reported temperature dependent changes were necessary but not sufficient by themselves (Figures 5 and 6 of the main document; see also Figure S4).

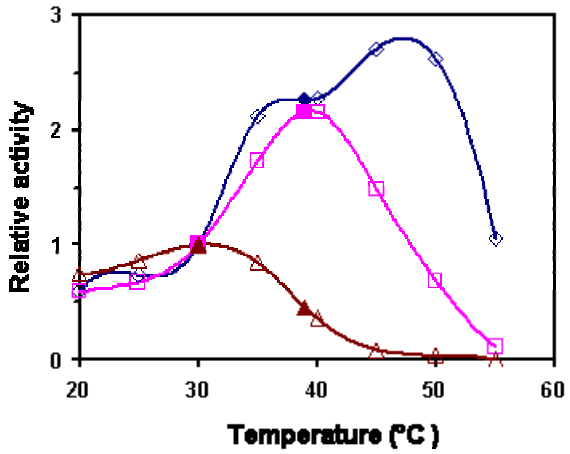

Figure S3 Effect of temperature on the activities of trehalase (△), trehalose 6-phosphate synthase (□) and trehalose 6-phosphate phosphatase (◇). The data were obtained from [3] and the lines are spline functions used to interpolate the experimental data. The solid symbols at 30ºC and 39ºC highlight the values used to calculate the Q_9=2.48, Q_{10}=2.35 and Q_{11}=0.42.

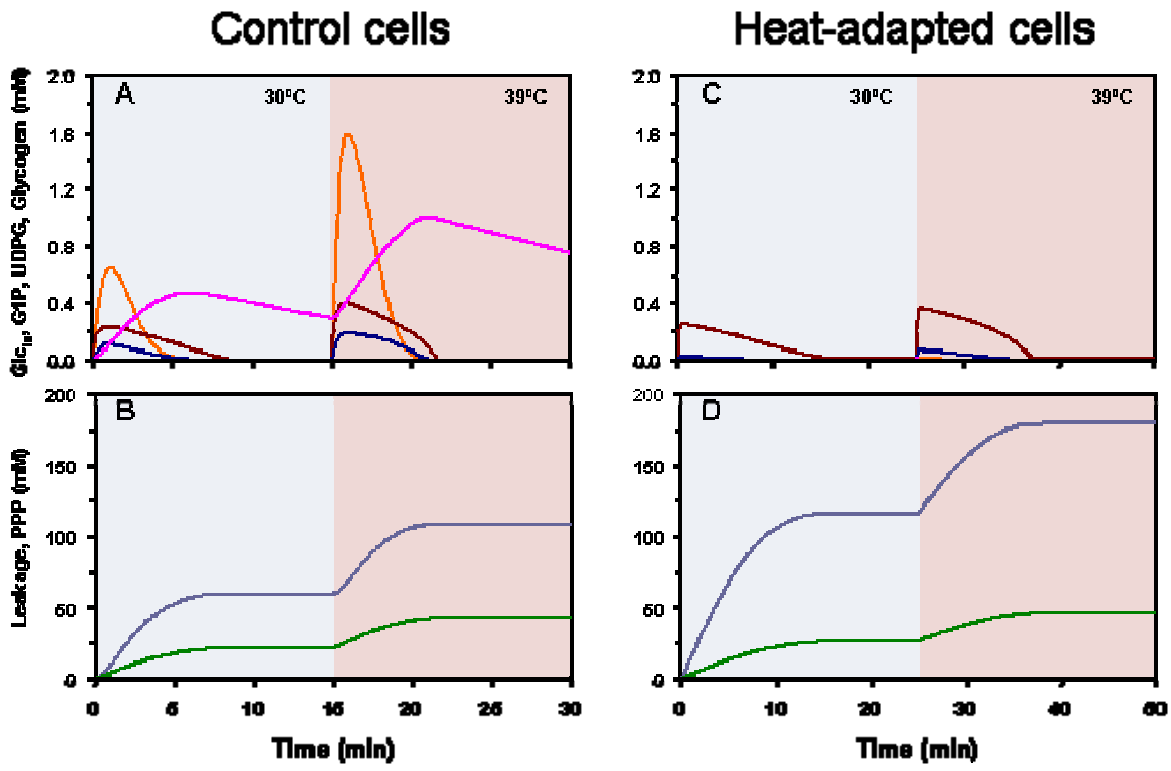

Figure S4 Model simulation of concentration trends for metabolites for which no experimental data are available and which are therefore not shown in Figure 5. Simulation of control cells (panels A and B), and heat-adapted cells (panels D and E) supplied with consecutive glucose pulses at 30ºC and at 39ºC. Temperatures: 30ºC ( ) and 39ºC ( ). Panels A and D: intracellular glucose (X_2, ——), glycogen (X_6, ——), G1P (X_4, ——) and UDPG (X_5, ——). Panels B and E: Leakage (X_{11},——) and PPP (X_{12}, ——).

Trehalose accumulation is an immediate response to heat stress

The results described in the main text suggest that, regardless of the working temperature, trehalose increases rapidly upon glucose addition. We were interested in establishing how quickly the trehalose level responds to an abrupt increase in temperature. To this end, an *in vivo* NMR experiment was performed with a continuous feed of [1-^{13}C]glucose (≈6.5 mM/min over 10 min) instead of a 65 mM pulse. During this steady supply of glucose, the temperature of the cell suspension was increased from 30ºC to 39ºC by quickly exchanging water-baths. Trehalose accumulation was detected as soon as the temperature reached 37ºC,

which took place within 2 min after switching water-baths (Figure S5). Therefore, the accumulation of trehalose observed in non-growing cells, in response to a sudden increase in temperature, cannot be dependent on transcriptional or translational regulation processes, which typically occur at a time scale of about 15 min [3], but are apparently the result of a direct effect of temperature on the activity of the enzymes that are responsible for the synthesis and degradation of trehalose.

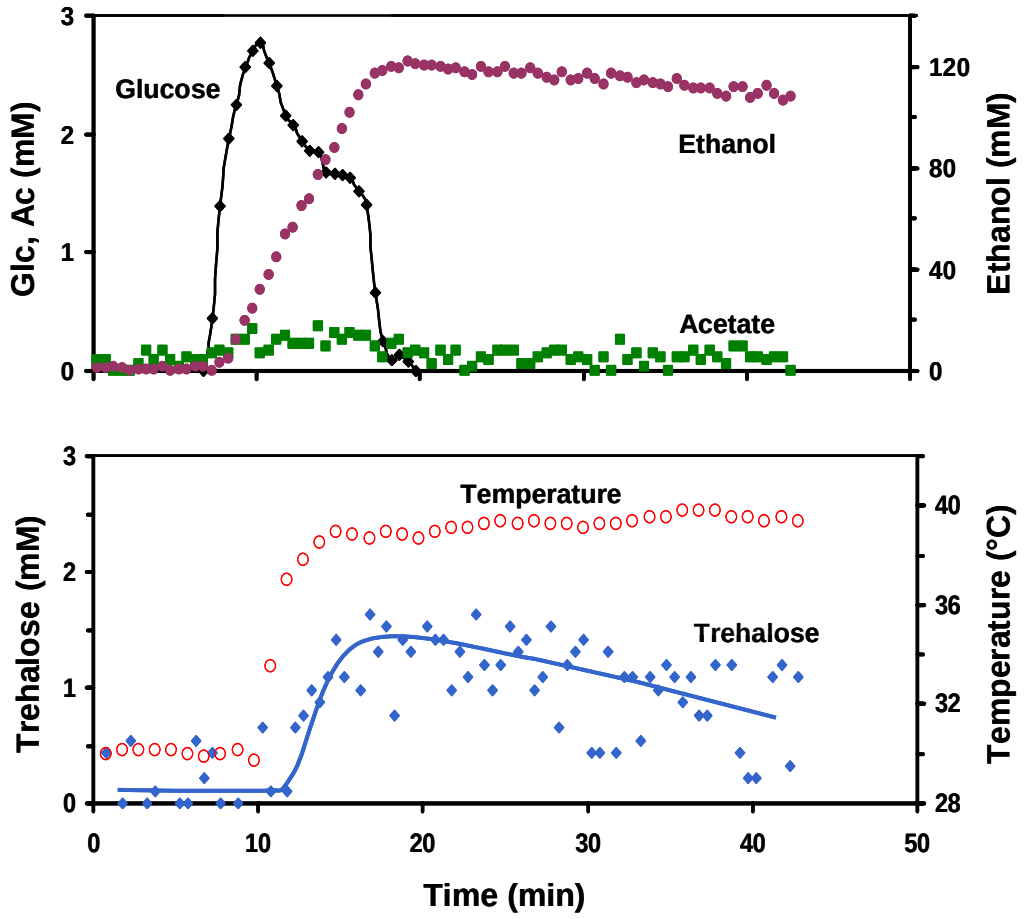

Figure S5 Metabolite time courses of non-growing *Saccharomyces cerevisiae* during a steady supply of glucose between $t = 7$ and $t = 17$, subjected to a temperature jump (30ºC → 39ºC) at $t = 10$. The upper panel shows the time courses of glucose (◆), ethanol (●), and acetate (■). The bottom panel shows trehalose (◆) and the temperature (○) profile of the cell suspension. The line visualizes the trend in trehalose concentration.

Flux ratio between glycolysis and the pentose phosphate pathway

NMR experiments with glucose labeled on carbon 2 allowed us to determine how much ethanol was produced directly through glycolysis or via the pentose phosphate pathway (PPP). Namely, the label on glucose ends up in C2 of ethanol when metabolism proceeds via glycolysis, and in C1 of ethanol when PPP is operating. The experiments were performed with cells grown under optimal temperature and showed that 5.5 ± 0.9% of the glucose was metabolized through the PPP at 30ºC and 4.8 ± 1.6% at 39ºC. Given that the results are not significantly different, a value of 5% was used for defining the magnitude of the PPP flux in the model (see Eq. 1 of the main text).

Model diagnostics

All parameter values in the model that were inferred from the time series data are in line with general experience with BST models over the past forty years (see [4]: Ch.5). Simulations furthermore revealed that the model is sufficiently robust against moderate variations in parameter values. The way that the model is set up, glucose is depleted, all internal variables approach zero, and ethanol and other output variables continue to increase as long as material flows through the system. Thus, the model has no non-trivial steady state that could be used for a typical sensitivity analysis. However, if the input is changed into a constant glucose influx, such as 5 mM, and if the accumulating output is not explicitly monitored with dependent variables, the system assumes a steady state that is asymptotically stable for both, control and heat-adapted cells, as is easily demonstrated with eigenvalue analysis. Furthermore, increasing the constant input in control cells by 10% leads to only modest absolute increases in most variables, except for glycogen and trehalose, which increase much more strongly, reflecting the observation that glycogen and trehalose are carbohydrate storage pools of the cell that can be used in times of need.

Experimental methods

Growth conditions

Cells were grown in a 5-liter fermentor. The pre-inocula were cultivated aerobically in shake-flasks at 30ºC under 200 RPM. Shake-flasks (250 ml) containing 80 ml of culture medium (G0 minimal medium [5] supplemented with 0.2% yeast extract) were inoculated with 300 µl of stock culture. Cells were grown for 14 hours until they reached an OD_{600} of 4.0. This culture was then used to inoculate a 5-liter fermentor (30ºC, 100 RPM, controlled pH 6.5 and continuous air flushing, pO_2 > 80%) to an initial OD_{600} of 0.04-0.05. Growth was monitored by optical density measurements at 600 nm and cells were harvested at an OD_{600} of 2.0. For the experiments with heat-adapted cells, cultures were prepared as described above, except that at an OD_{600} of 1.3, the temperature was increased to 39ºC (heat shock conditions) and cells allowed to grow for further 40 min until an OD_{600} of 2.0 was reached.

In vivo ^{13}C-NMR experiments

Cells were harvested during the mid-exponential growth phase (OD_{600} of 2.0), centrifuged (10 min, 8600×*g*, 4ºC), washed once with 5 mM potassium phosphate buffer (KP_i) pH 6.5, and re-suspended in 50 ml of 50 mM KP_i buffer (pH 6.5), containing 6 % (v/v) ^2H_2O and antifoam agent. The cell suspension was transferred to a 100-ml bioreactor connected to a 10-mm NMR tube by a circulating system [6]. The cell suspension was circulated at a rate of 30 ml/min by using peristaltic pumps; to minimize pulsation and to achieve a constant flow, a two-pump system was used to circulate the suspension from the bioreactor to the NMR tube. A controller was used to maintain temperature (at 30ºC or 39ºC), pH (at 6.5) (pH electrode Crison instruments, SA, Barcelona, Spain) and pO_2 (>80%) (pO_2 electrode Mettler Toledo, Spain). pH was maintained by addition of 4 M NaOH or 2 M HCl. pO_2 was maintained by bubbling oxygen through the cell suspension in the bioreactor and injecting O_2 in the head-

space of the NMR tube. Control spectra were acquired for a few minutes (<5 min) prior to the addition of a glucose pulse (0.585 g of [1-^{13}C]glucose). The initial glucose concentration was approximately 65 mM. Consecutive ^{13}C-NMR spectra were acquired for the total length of the experiment (typically 2 hours) to monitor glucose consumption, intracellular metabolites, and end-products. After glucose depletion, a period of 15-20 min was allowed until the pH of the suspension reached a constant value: this delay is necessary because the pH of the culture tends to increase after glucose depletion due to release of CO_2, an end-product of fermentation. After this period, the temperature was shifted from 30°C to 39°C. Once the temperature was stabilized (3-5 min), a new pulse of glucose was supplied. The same procedure was executed, but in this case the temperature was shifted back to 30°C and a third pulse of glucose was supplied.

While this procedure constituted the basic experimental setup, some experiments were performed with other glucose isotopomers ([2-^{13}C]glucose and [6-^{13}C]glucose) to measure the ratio of fluxes via glycolysis and the pentose phosphate pathway, and to optimize the NMR analysis of glucose-6P and trehalose-6P, respectively. In other NMR experiments three consecutive pulses of glucose were added while keeping the temperature at 39°C (heat stress conditions). Additionally, we performed experiments in which [1-^{13}C]glucose (0.585 g) was added slowly over 10 min instead of as a single pulse. In this case, the temperature was increased to 39°C at time 3 to 4 min after the start of adding glucose.

^{13}C-NMR spectroscopy

All NMR spectra were run with a quadruple-nucleus probe head on a Bruker DRX500 spectrometer at 30ºC or 39ºC. *In vivo* ^{13}C-NMR spectra were acquired as previously described [6], for time periods up to 2 hours. For the quantification of metabolites, correction factors were used to account for saturation and nuclear Overhauser effects. These factors were

calculated as the ratio of the resonances areas obtained under fully relaxed and saturated conditions (recycle delays of 1.5 s and 60.5 s, respectively), for the metabolites of interest.

Quantification of intracellular metabolites in living cells by ^{13}C-NMR

Quantitative kinetic data were calculated from the areas of the respective resonances by applying appropriate correction factors and comparing with the intensity of an internal concentration standard, tetramethylurea. Intracellular metabolite concentrations were calculated considering a value of 2.38 μl of yeast cell volume per mg dry weight [7; 8].

Modeling methods

Model design

As always in BST, all reactions were modeled as products of power-law functions, but a key difference to earlier models of the trehalose pathway was the method of parameterization. While all prior models had used a bottom-up approach based on kinetic data from the literature and a number of explicit and implicit assumptions, we performed *in vivo* ^{13}C-NMR time series experiments and used a top-down method for estimating the unknown parameter values directly from the new data.

It is very rare for dynamic metabolic models to account explicitly for temperature. Because temperature is an obviously crucial driver in investigations of heat stress, we expanded the typical GMA format with the inclusion of temperature, as well as other factors that changed directly in response to temperature.

Under the *in vivo* NMR conditions, the cells were suspended in phosphate buffer to high cell density (≈ 200 OD, 60 mg/ml of dry weight) and fed short pulses of glucose. We therefore assumed no growth and no changes in protein levels during the time series measurements.

The differential equation model with the above settings was implemented and solved in MATLAB™ (Mathworks). The kinetic parameters were obtained by performing nonlinear optimization, using a weighted sum of squared residuals as objective function. Initial values were specified based on experience with BST systems. Parameter values are presented in Tables 1, S1 and S2. For comparisons, the model was also implemented in the freeware PLAS [2] (see Box S2).

Similarity of Time Courses

An obvious question with experiments in biology is repeatability. While there are abundant statistical techniques for steady-state data, a rigorous statistical analysis of results from time series experiments is complicated. In order to give an impression of the similarity of time courses, Figure S6 shows results obtained for four replicates of our substrate bolus standard experiment. Because time series experiments incur variability arises along both, the X- and Y-axes, the temporal profiles were normalized in the time domain for biomass. Specifically, the temporal dimension of each experiment *j* was multiplied by the specific biomass observed in the experiment and divided by the average biomass of the four replicates ($t_{ij} \cdot B_j / \overline{B}$). This normalization allows a biomass-adjusted superimposition of the concentration time series from experiments with different uptake profiles. Figure S6 shows that the results do not differ much between experiments. Nonetheless, averaging measurement points in time would not be straightforward, because of variation in time and concentration. For these reasons it was deemed more appropriate to develop the model fits with representative rather than average profiles.

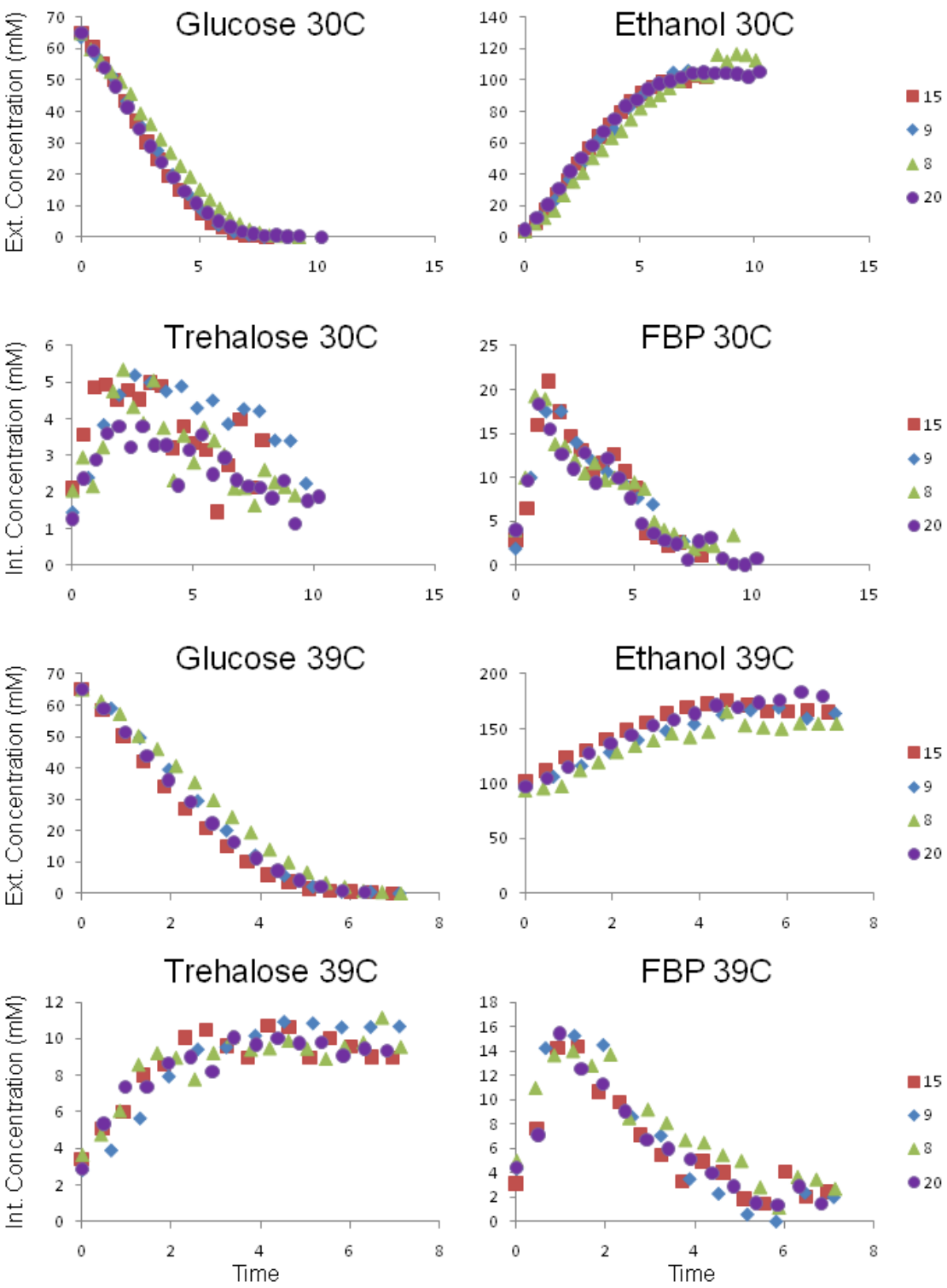

Figure S6 Metabolite time courses of four independent experiments (replicates), showing the profiles of glucose, ethanol, trehalose and FBP at 30°C and 39°C. Time was normalized for biomass, as explained in the text.

Supplementary tables

Table S1 Model parameters (rate constants and kinetic orders) obtained from *de novo* time series data by means of optimization

Flux	Model step	Rate constant	Kinetic orders for substrates	Kinetic orders for regulators***
1	HXT	$2.87*10^{-5}$	$0.526^{(30ºC)*}$ $0.472^{(39ºC)*}$	$-0.002^{(G6P)}$
2	HXK	$1.90*10^{-4}$	0.510	$-0.209^{(Tre6P)}$
3	PGM^F	$5.66*10^{-6}$	0.400	
4	PGM^R	$3.13*10^{-5}$	0.471	
5	UGP^F	$3.58*10^{-5}$	0.767	
6	UGP^R	$1.31*10^{-5}$	0.159	
7	GSY	$9.43*10^{-7}$	0.459	$0.000^{(G6P)}$
8	GPH	$6.94*10^{-8}$	0.311	$-0.002^{(G6P)}$ $-0.001^{(UDPG)}$
9	TPS1	$1.19*10^{-6}$	$0.659^{(G1P)**}$ $0.625^{(UDPG)**}$	$-0.000^{(Glc)}$
10	TPS2	$3.24*10^{-6}$	0.361	
11	NTH	$1.99*10^{-7}$	0.082	
12	PFK	$2.89*10^{-5}$	0.693	
13	"FBA"	$6.13*10^{-5}$	0.369	
14	Leakage	$5.54*10^{-6}$	0.672	

"FBA" designates the collection of enzymatic steps between fructose 1,6-bisphosphate aldolase and the release of end-products;
* Superscripts show the temperature of the kinetic order for glucose transport; ** Superscripts indicate the substrate associated with each kinetic order; *** Superscripts show the regulating metabolite.

Table S2 Comparison of temperature coefficients (Q) obtained from the model with published temperature effects on corresponding enzymatic activities

Flux	Model step	Q	Ratio of enzyme activity at 30 and 38ºC**
1	HXT	1.57	1.1 (1.1)
3	PGM^F	1.48	nd
9	TPS1	2.48^*	nd
10	TPS2	2.35^*	nd
11	NTH	0.42^*	nd
13	"FBA"	1.26	0.7-1.7 (0.6-1.9)

*From [3]. ** Data from [9]. Parentheses show the values calculated for the respective temperature coefficients Q_{10}.
nd: not determined. "FBA" designates the enzymatic steps lumped between FBA and the release of glycolytic end-products.

Box S2: PLAS file of the complete model

```
x1=65
x2=.01
x3=.01
x4=.01
x5=.01
x6=.01
x7=.01
x8=.01
x9=.01
x10=3
x11=.01
x12=.01

T=30 // Temperature of the experiment
T9=1
T10=1
T11=1
TDW=TDWn
Vi=Vin
GT=1
g1=gx1

@ 15 T=39
@ 15 x1=65
@ 15 x8=.7
@ 15 T9=2.2629
@ 15 T10=2.1562
@ 15 T11=0.45361
@ 15 g1=gx16
@ 15 GT=1
@ 15 TDW=TDWn
@ 15 Vi=Vin

@ 50 T=30
@ 50 GT=2
@ 50 TDW=TDWh
@ 50 Vi=Vih
@ 50 x1=65
@ 50 x2=.01
@ 50 x3=.01
@ 50 x4=.01
@ 50 x5=.01
@ 50 x6=.01
@ 50 x7=.01
@ 50 x8=.01
@ 50 x9=.01
@ 50 x10=3
@ 50 x11=.01
@ 50 x12=.01
@ 50 T9=1
@ 50 T10=1
@ 50 T11=1
@ 50 g1=gx1

@ 75 T=39
@ 75 GT=2
@ 75 TDW=TDWh
@ 75 Vi=Vih
@ 75 x1=65
```

```
@ 75 x8=8.15
@ 75 T9=2.2629
@ 75 T10=2.1562
@ 75 T11=0.45361
@ 75 g1=gx16

q1=tc1^((T-30)/10)
q3=tc2^((T-30)/10)
q13=tc3^((T-30)/10)

!! x1 x2 x3 x4 x5 x6 x7 x8 x9 x10 x11 x12 T

X1 =(abs[10^-8 +x1+abs[x1]]/2)
X2 =(abs[10^-10 +x2+abs[x2]]/2)
X3 =(abs[10^-8 +x3+abs[x3]]/2)
X4 =(abs[10^-10 +x4+abs[x4]]/2)
X5 =(abs[10^-12.5 +x5+abs[x5]]/2)
X6 =(abs[10^-9 +x6+abs[x6]]/2)
X7 =(abs[10^-8 +x7+abs[x7]]/2)
X8 =(abs[10^-8 +x8+abs[x8]]/2)
X9 =(abs[10^-8 +x9+abs[x9]]/2)
X10 =(abs[10^-8 +x10+abs[x10]]/2)
X11 =(abs[10^-8 +x11+abs[x11]]/2)
X12 =(abs[10^-8 +x12+abs[x12]]/2)

// Fluxes
F1=TDW*e1   *X1^g1  *X3^gr1         *GT^P1  *q1       // HXT
F2=TDW*e2   *X2^gx2 *X7^gr2         *GT^P2            // HXK1/2, GLK
F3=TDW*e3   *X3^gx3                 *GT^P3  *q3       // PGM1/2 f
F4=TDW*e4   *X4^gx4                 *GT^P4            // PGM1/2 r
F5=TDW*e5   *X4^gx5                 *GT^P5            // UGP1 f
F6=TDW*e6   *X5^gx6                 *GT^P6            // UGP1 r
F7=TDW*e7   *X5^gx7 *X3^gr3         *GT^P7            // GSY1
F8=TDW*e8   *X6^gx8 *X3^gr4 *X5^gr5 *GT^P8            // GPH1 f
F9=TDW*e9   *X3^gx9 *X5^gx10*X2^gr6 *GT^P9  *T9       // TPS1
F10=TDW*e10 *X7^gx11                *GT^P10 *T10      // TPS2
F11=TDW*e11 *X8^gx12                *GT^P11 *T11      // NTH1/2
F12=TDW*e12 *X3^gx13                *GT^P12           // PFK1/2
F13=TDW*e13 *X9^gx14                *GT^P13 *q13      // FBA
F14=TDW*e14 *X9^gx15                *GT^P14           // Sink
F15=0.05*F12                                          // ZWF1


// Diff. eq.
x1'=-F1/Ve                                  // Glc Ext
x2'=(F1+2*F11-F2)/Vi                        // Glc in
x3'=(F2+F4-F3-F9-F12-F15)/Vi                // Glc-6P
x4'=(F3-F4+F6-F5+F8)/Vi                     // Glc-1P
x5'=(F5-F6-F7-F9)/Vi                        // UDP-Glc
x6'=(F7-F8)/Vi                              // Glycogen
x7'=(F9-F10)/Vi                             // Tre-6P
x8'=(F10-F11)/Vi                            // Tre
x9'=(F12-F13-F14)/Vi                        // FBP
x10'=2*F13/Ve                               // Final Prod. Eth+Gly+Ace
x11'=F14/Vi                                 // Sink
x12'=F15/Vi                                 // PPP

t0=0
tf=100
hr=1
```

```
e1    =     2.87E-05
e2    =     1.90E-04
e3    =     5.66E-06
e4    =     3.13E-05
e5    =     3.58E-05
e6    =     1.31E-05
e7    =     9.43E-07
e8    =     6.94E-08
e9    =     1.19E-06
e10   =     3.24E-06
e11   =     1.99E-07
e12   =     2.89E-05
e13   =     6.13E-05
e14   =     5.54E-06
gx1   =     5.26E-01
gx2   =     5.10E-01
gx3   =     4.00E-01
gx4   =     4.71E-01
gx5   =     7.67E-01
gx6   =     1.59E-01
gx7   =     4.59E-01
gx8   =     3.11E-01
gx9   =     6.59E-01
gx10  =     6.25E-01
gx11  =     3.61E-01
gx12  =     8.22E-02
gx13  =     6.93E-01
gx14  =     3.69E-01
gx15  =     6.72E-01
gx16  =     4.72E-01
gr1   =     -1.94E-03
gr2   =     -2.09E-01
gr3   =     3.50E-04
gr4   =     -2.24E-03
gr5   =     -1.21E-03
gr6   =     -4.05E-04
tc1   =     1.57E+00
tc2   =     1.48E+00
tc3   =     1.26E+00
P1    =     -5.51E-01
P2    =     3.20E+00
P3    =     4.37E+00
P4    =     4.11E+00
P5    =     4.02E+00
P6    =     4.70E+00
P7    =     -1.69E-01
P8    =     5.95E+00
P9    =     4.42E+00
P10   =     3.83E+00
P11   =     2.29E+00
P12   =     6.50E-03
P13   =     3.19E-01
P14   =     2.05E+00

TDWn=60.25*Ve*1000
Vin=2.38*TDWn/1000/1000
TDWh=48.2*Ve*1000
Vih=2.38*TDWh/1000/1000
Ve=50/1000
```

References

[1] R. Castro, A.R. Neves, L.L. Fonseca, W.A. Pool, J. Kok, O.P. Kuipers, and H. Santos, Characterization of the individual glucose uptake systems of Lactococcus lactis: mannose-PTS, cellobiose-PTS and the novel GlcU permease. Mol Microbiol 71 (2009) 795-806.
[2] A.E.N. Ferreira, www.dqb.fc.ul.pt/docentes/aferreira/plas.html. (1996).
[3] M.J. Neves, and J. François, On the mechanism by which a heat shock induces trehalose accumulation in *Saccharomyces cerevisiae*. Biochem J 288 (Pt 3) (1992) 859-64.
[4] E.O. Voit, Computational Analysis of Biochemical Systems: A Practical Guide for Biochemists and Molecular Biologists, Cambridge University Press, New York, 2000.
[5] W.W. Hauswirth, Lim, L.O., Dujon, B., Turner, G. , Methods for studying the genetics of mitochondria. in: V.M. Darley-Usmar, Rickwood, D., Wilson, M. T., (Ed.), Mitochondria: a practical approach., IRL Press, 1987, pp. 171-244.
[6] A.R. Neves, A. Ramos, M.C. Nunes, M. Kleerebezem, J. Hugenholtz, W.M. de Vos, J. Almeida, and H. Santos, *In vivo* nuclear magnetic resonance studies of glycolytic kinetics in *Lactococcus lactis*. Biotechnol Bioeng 64 (1999) 200-12.
[7] G. Ditzelmüller, W. Wöhrer, C.P. Kubicek, and M. Röhr, Nucleotide pools of growing, synchronized and stressed cultures of *Saccharomyces cerevisiae*. Arch Microbiol 135 (1983) 63-7.
[8] U. Theobald, W. Mailinger, M. Baltes, M. Rizzi, and M. Reuss, *In vivo* analysis of metabolic dynamics in *Saccharomyces cerevisiae*: I. Experimental observations. Biotechnol Bioeng 55 (1997) 305-16.
[9] J. Postmus, A.B. Canelas, J. Bouwman, B.M. Bakker, W. van Gulik, M.J. de Mattos, S. Brul, and G.J. Smits, Quantitative analysis of the high temperature-induced glycolytic flux increase in *Saccharomyces cerevisiae* reveals dominant metabolic regulation. J Biol Chem 283 (2008) 23524-32.